THREE DIMENSIONAL NUMERICAL MODEL OF AQUIFER FOR SPRINGS AND HOT SPRINGS IN KARANG VOLCANIC AREA, WEST JAVA, INDONESIA

A.Harada[1], R.Itoi[1] and B.Yoseph[1]

[1] Department of Earth Resources Engineering, Faculty of Engineering, Kyushu University,

Motooka 744, Nishi-ku, Fukuoka 819-0395, Japan

a-harada@mine.kyushu-u.ac.jp

Keywords: *Groundwater, numerical simulation, hot spring, spring, Mt.Karang, Mt.Parakasak*

ABSTRACT

The study area is located in west Java where there are two mountains: Mt. Karang and Mt. Parakasak. Geological components of this area are mostly volcanic products such as pyroxene andesite, tuff, volcanic breccia, and basaltic lava.

Both cold springs and hot springs are located on the northern foot of these mountains at the same elevation, but hot springs mainly discharge in the western part of this area: on the foot of Mt. Parakasak. Both types of springs seem to be located along a fault system running east to west in this area. A three-dimensional aquifer model was developed to understand fluid and heat transports in the aquifer and to explain the presence of cold springs and hot springs.

Development of the model and numerical simulation were carried out using the FEFLOW numerical simulator. The model covers an area of about 180km^2, and consists of 21 layers. The thickness of each layer is 0-160m, depending on the location. A high temperature zone of 100^{o}C was assigned in the bottom layer below Mt.Parakasak, and 50-56^{o}C discharge was obtained in the model in the area where the hot springs are located. On the other hand, a 25-26^{o}C discharge was obtained for the cold springs. The groundwater flows mainly from south to north. Therefore, the groundwater heated below Mt. Parakasak forms hot spring at the foot of the mountain.

1. INTRODUCTION

Utilization of geothermal energy is growing all over the world. An estimate of the installed geothermal energy for direct utilization at the end of 2009 is 48,493 MWt (Lund et al.,-2011). One of the traditional and common direct uses of geothermal heat is bathing in hot springs. Hot springs are important for tourism and for enhancing the lifestyle of local residents .

Mt. Karang amd Mt. Parakasak are volcanoes in west Java, Indonesia, and both hot springs and cold springs are present on the northern flank of these mountains. Groundwater resources in this area play an important role for local communities for agriculture and daily uses as well as local industry. At the same time, geothermal resources can be used for direct heat use and bathing. In order to make the best use of groundwater and geothermal energy, a modeling study need to be made for designing the optimal use of these resources. Thus, a three dimensional modeling study was conducted of underground water flow and heat transport in the aquifer in order to understand the groundwater and geothermal systems in this area.

2. FIELD DATA

2.2 Geological data

Figure 1 shows the location of the study area. It is about 160km west from Jakarta, the capital of Indonesia.

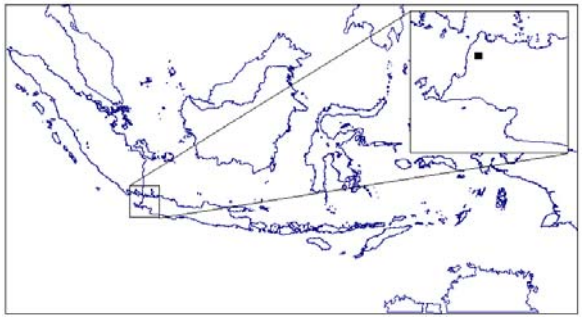

Figure 1: Location of the study area

Figure 2 shows a geological map of the study area. It mostly consists of volcanic products that can be divided into five categories as follows: Rawa Danau sediments, Mt. Karang volcanic products, Mt. Parakasak volcanic products, Mt. Kamuning volcanic products and old volcanic products. Lapilli tuff, white to brownish-red, containing of fairly abundant pumice fragments cover a large part of Mt. Parakasak. There are andesitic to basaltic lava, porphyritic, sheeting joints structure and vesicular texture at high elevations on Mt. Karang, and pyroxene andesite-basalt, jointed, cavernous at the low elevations of Mt. Karang. The solid line in Fig. 2 represents a confirmed fault while dotted lines represent estimated faults. Three faults out of five run from northeast to southwest. Although the geology at the surface varies in the horizontal direction, it is simplified in the model. However, the detailed geology was considered in deciding the properties of the model.

2.2 Water sampling

Geochemical study of waters in this area was conducted by Yoseph *et al*. (2012). Figure 3 presents the locations of sampling points, and Table 1 shows the measured temperatures. In Fig. 3, an open circle represents the location of a cold spring, a solid circle a hot spring, gray open circle a river and a cross in an open circle a well. The temperature of the hot springs ranges from 40 to 61^{o}C. Figures 2 and 3 indicate that cold springs and hot springs seem to be located along fault systems.

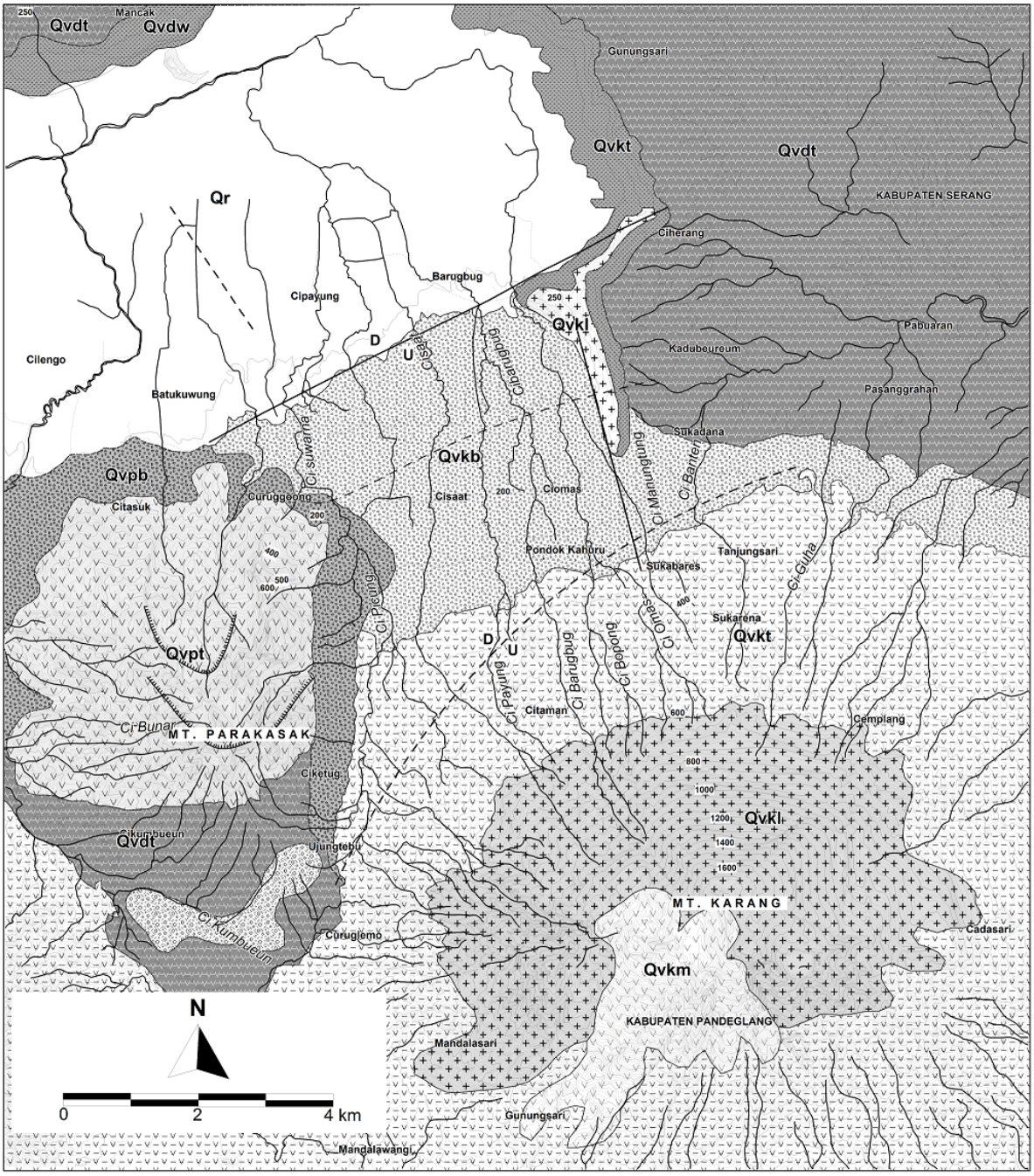

Mt. Karang Volcanic Product

Qvkm	Pyroxene andesite - basalt, jointed, cavernous
Qvkl	Andesitis to basaltic lava, phorphyritic, sheeting joints structure and vesicular texture
Qvkt	Tuff, yellow to brownish and reddish brown colour, fine grained, solid
Qvkb	Volcanic breccia, brownish - yellowish. Components consist of andesitis - basaltic rock, matrix supported.

Mt. Parakasak Volcanic Product

Qvpt	Lapilli tuff , white to brownish-red, containing of fairly abundant pumice fragments.
Qvpb	Volcanic breccia, brownish color. Components consist of andesitis - basaltic rock, matrix supported

Mt. Kamuning Volcanic Product

Qvkl	Andesitis to basaltic lava, sheeting joints structure and vesicular texture
Qvkt	Tuff, light gray - dark gray, fine to coarse, massive, moderately sorted.

Old Volcanic Product

Qvdt	Tuff, light gray - dark gray, fine to coarse, massive, moderately sorted.
Qvdw	Weathered tuff, part of the ancient volcanic lake product

Rawa Danau Sediment

Qr	Sediment consist of clay, silt, sandy gravel, and pumice.

Figure 2: Geological map

Table 1: Measured temperatures of water samples

Sample ID	Object Observ.	Temperature (°C)
KR-1	spring	24.1
KR-2	spring	25.4
KR-3	spring	24.9
KR-4	spring	26.9
KR-4C	spring	25.6
KR-5	hot spring	60.9
KR-6	hot spring	54.0
KR-7	hot spring	54.4
KR-8	hot spring	55.7
KR-9	hot spring	42.0
KR-10	hot spring	51.6
KR-11	river	25.8
KR-12	river	25.0
KR-13	spring	24.8
KR-14	river	27.4
KR-15	spring	24.3
KR-16	river	25.0
KR-17	river	25.1
KR-18	river	23.6
KR-19	spring	23.3
KR-20	river	27.9
KR-21	spring	23.5
KR-22	river	27.0
KR-23	river	27.3
KR-24	spring	25.1
KR-25	spring	22.3
KR-26	spring	22.7
KR-27	spring	22.2
KR-28	spring	22.7
KR-29	spring	25.2
KR-30	dug well	22.0
KR-31	spring	24.9
KR-32	spring	24.9
KR-33	spring	25.1
KR-34	spring	25.2
KR-35	dug well	24.4

2.3 Electric resistivity surveys

Electric resistivity surveys were conducted in the study area by Cipta et al. (2011). Figure 4 shows the survey lines. The area shown in Fig. 4 corresponds to that of the three dimensional model developed in this study. Blue line denotes the survey lines of electric resistivity surveys, and black line the elevation contours. The number of observation points is 105. The results of electric resistivity surveys at 105 points were analyzed and then integrated into a two dimensional resistivity contour map (Figure 7) by means of inverse analysis.

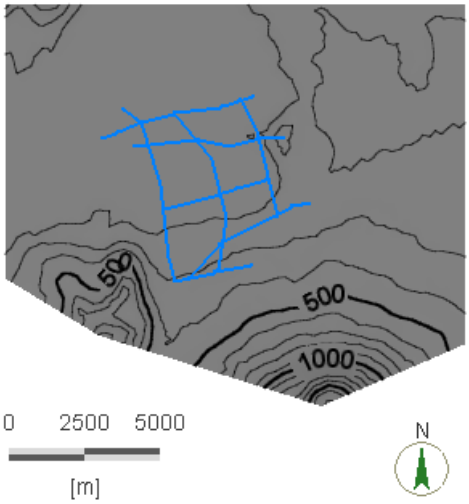

Figure 4: Resistivity survey lines

3. NUMERICAL MODEL

3.1 Development of the model

Based on the data in discussed in Section 2, a three dimensional aquifer model for flow of water and energy was constructed. As shown in Fig.5, the model extends 15191m in the east-west direction, and 13241m in the north-south direction. The number of layers is 21. The model extends from the surface to 300m below sea level. The number of elements per layer is 5981, giving a total of 125601 elements. Most of elements have a dimension of about 250m on a side. The elements near where hot spring are located were refined and they are about 5m on a side.

The layers have a different thickness, ranging from 0-160m. The thickness of the layers is determined based on the results of the electrical resistivity surveys. Although the geology at the surface varies in the horizontal direction, it is simplified in the model. The layer thickness at places outside of the survey lines is interpolated by the inverse distance method (Olena, B., Clayton, V.D., 2009). This is one of the most commonly used techniques for interpolation of scattered points. The inverse distance weighted method is based on the assumption that the interpolating surface should be influenced most by the nearby points and less by the more distant points.

Table 2 summarizes thermal and hydraulic properties of each layer. These values were determined by considering information on rock types, results of the resistivity distribution and drilling core (Yoseph *et al.*, 2012). Hydraulic conductivities in the vertical and horizontal directions were given the same value except at the places where hot springs and cold springs occur where it was set at 10^{-3} m/s in the vertical direction. These values were determined on the basis of values for similar rock types in the references (Bear J., 1979; De Wiest, 1969; Fetter.C.W., 1994).

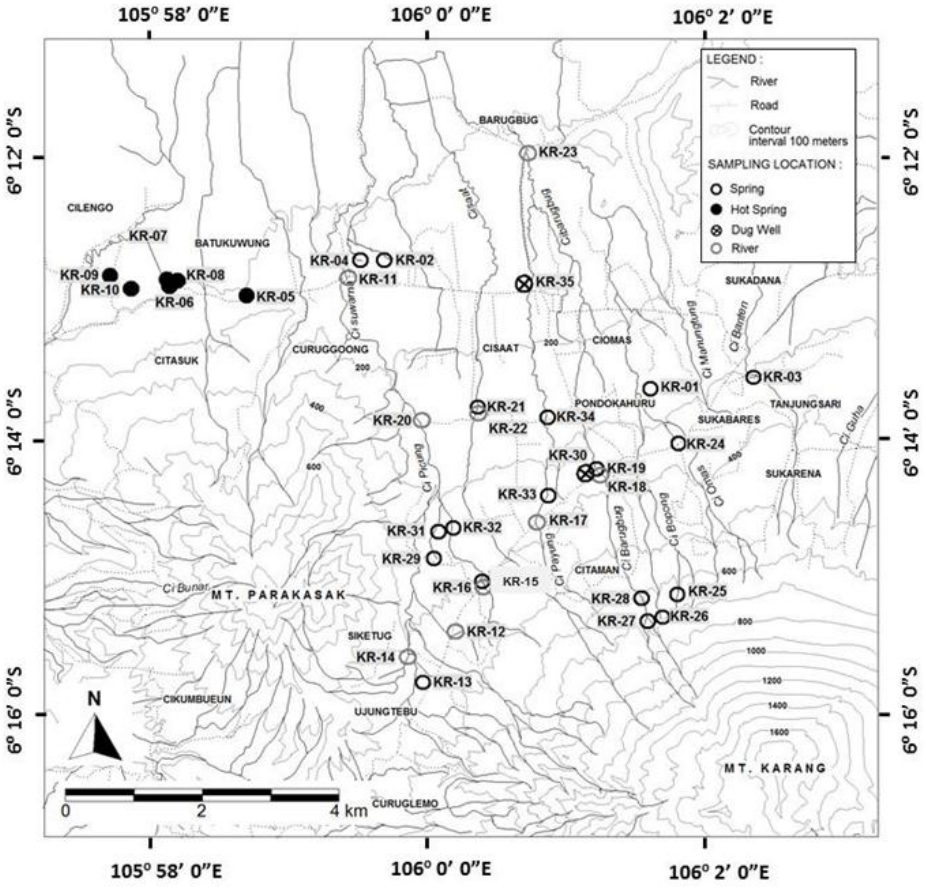

Figure 3: Sampling locations

Table 2: Hydraulic and thermal properties given for elements.

	Porosity (%)	Horisontal conductivity (m/s)	Heat conductivity (W/m/K)
Layer 1	20	10^{-4}	1.9
Layer 2-13	5	10^{-10}	2.3
Layer 14	20	10^{-4}	1.9
Layer 15	5	10^{-10}	2.3
Layer 16	20	10^{-4}	1.9
Layer 17-21	3	10^{-11}	2.6

3.2 Numerical simulation

Initial conditions and boundary conditions were set based on simplified assumption. The initial condition for the underground water flow is that hydraulic head is 70% of the surface elevation at each node of the element except for the points corresponding to hot springs and cold springs. At the nodes for the hot springs and cold springs, the value of hydraulic head is same as the surface elevation. This is because water is discharging at these points.

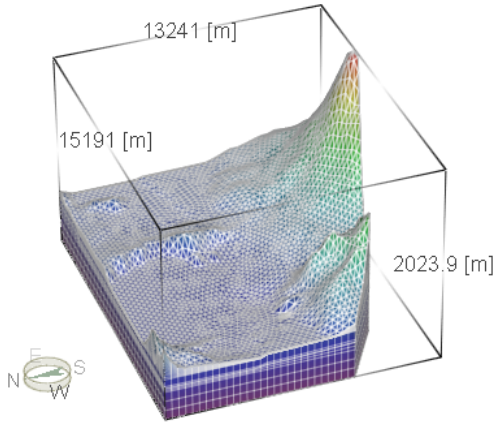

Figure 5: A bird-eye view of the model

The initial condition for heat transport is that air temperature at the surface depends on elevation. The surface air temperature was calculated as follows:

$$T = 27 - \{\ 0.007 \times \text{elevation (m)}\ \}\ (^{o}C)$$

The initial temperature in the whole domain was set at 27°C .

The boundary conditions for the underground water flow were set as follows. In general, hydraulic head and temperature are specified at nodes of the model. At the surface of the model, the hydraulic head is set as 70% of the surface elevation except for the nodes corresponding to hot springs and cold springs. The hydraulic head at the nodes of hot springs and cold springs is the same as that of the surface elevation because there is discharge of water there. This is same as for the initial conditions. The hydraulic head of the lateral boundaries at both the northern and southern sides is set at 70% of the surface elevation. Whereas the boundaries in the east and west are taken to be impermeable. In addition, the bottom of the model is also treated as impermeable. Therefore, the Darcy flux is 0 m/day. Thus in this case, the upflow from the deeper geothermal resource is not included. The recharge of the system is simulated by fixing the hydraulic head at some boundaries.

Heat transfer between the surface of the model and the atmosphere was taken into account. The air temperature was calculated by the same equation as the one used to calculate intial temperatures at the surface of the model. All lateral boundaries are assumed to be adiabatic, and hence the value of heat flux is 0 J/m^2/day. The temperature at the bottom of the model is set at 100^{o}C below Mt. Parakasak and 50^{o}C at other nodes.

These values were varied until a good match for the hot springs was achieved

The model was run with the FEFLOW numerical simulator (Diersch, 2002) for 3.65x10^8 day of simulation time to achieve a steady state.

3.2 Results and discussion

Results of the simulation indicate that underground water mainly flows from south to north. Because of this, underground water is heated below Mt. Parakasak and flows towards the foot of the mountain. Then the heated water flows upward through fractures and discharges at the surface.

Although there are no measured data to compare with, the calculated horizontal velocity of groundwater in the permeable layers ranges between 3.0x10^{-5} m/s and 1.5x10^{-6} m/s below the mountain. The calculated horizontal velocity in permeable layers in the plain area range 1.5×10^{-6} m/s and 1.3x10^{-8}m/s. The velocity of upflow in the area where there are hot springs and cold springs ranges from 1.6x10^{-3} m/s to 2.7x10^{-3} m/s, and this is rather high compared to the horizontal velocity.

Figure 6 shows temperature distributions at the surface, 90m, -70m and -150m above sea level.

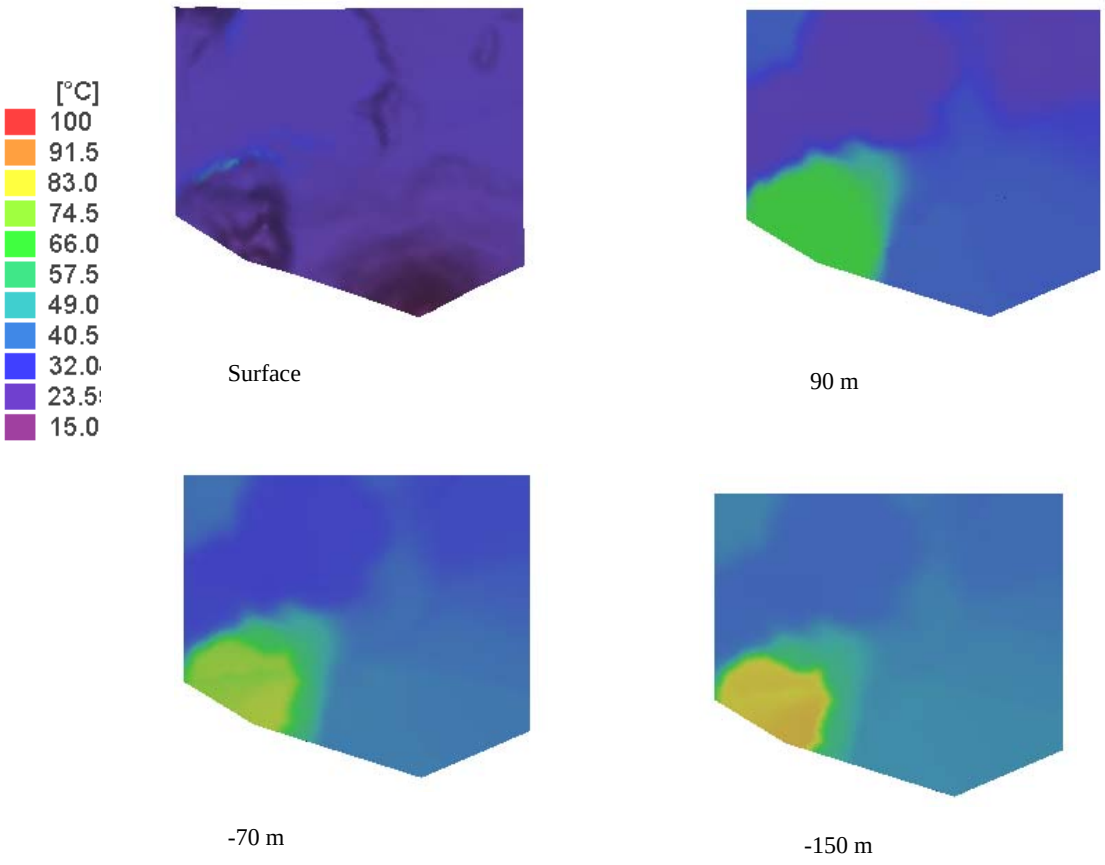

Figure 6: Temperature distribution at different layers

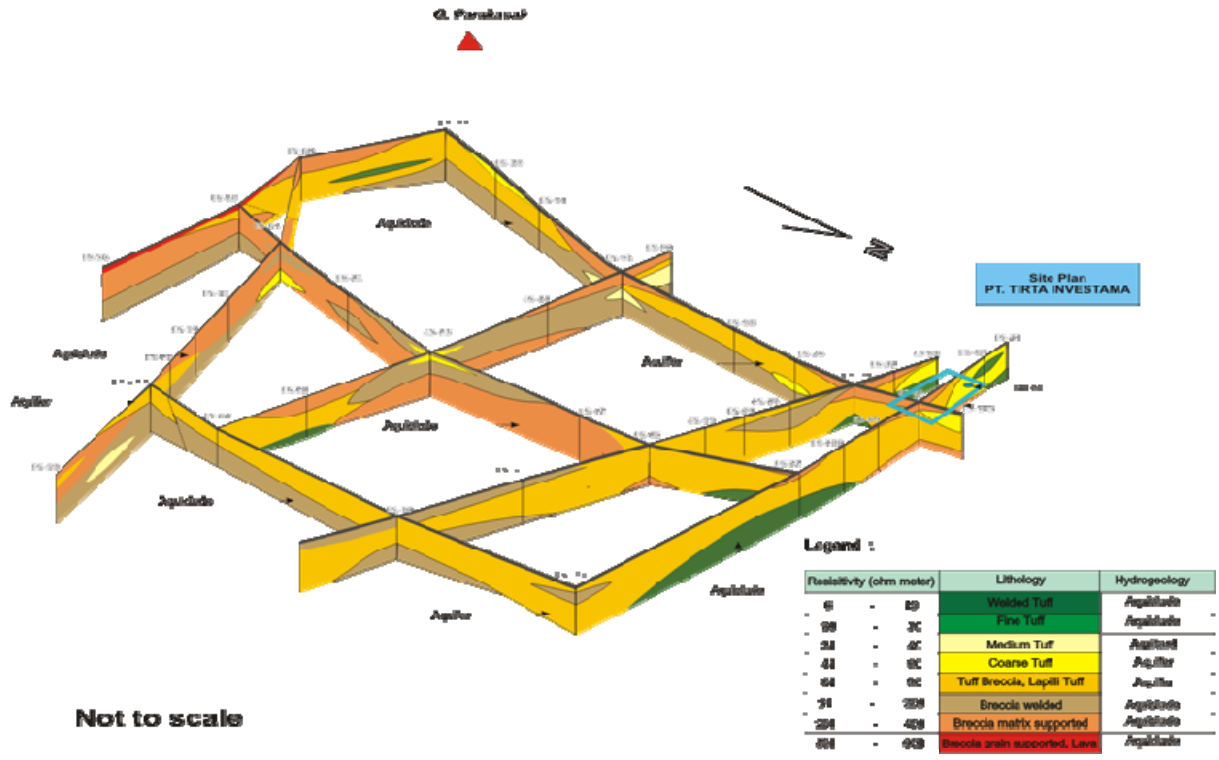

Figure 7: Two dimensional resistivity contour map

These four figures also show the temperature change with elevation. As the figures show, temperature in the area where the hot springs are found is higher than that in the surrounding area. The temperature of discharging water range from 50 ^{o}C to 56 ^{o}C. On the other hand, a discharge ranging from 25 ^{o}C to 26 ^{o}C was obtained in the simulation in the area where the cold springs are located. These values agree well with measured temperatures. Although there are no measured data to compare with, the discharge rate of each hot spring and cold spring is calclated to be between $3.43x10^{-2}$ m^3/s and $5.79x10^{-2}$ m^3/s.

4. CONCLUSIONS

A three dimensional numerical model of an aquifer for cold springs and hot springs in the study area of Mt. Karang volcanic area in West Java, Indonesia was developed to assist with understanding underground water flow and heat transport. The model was developed on the basis of the data from geology and electric resistivity surveys. The thickness of layers is determined based on the results of electrical resistivity surveys. Although the geology at the surface varies in the horizontal direction, it is simplified in the model. The layer thickness at places outside of the survey lines is interpolated by the inverse distance method. The model was used for numerical simulations of underground water flow and heat transport. The simulated results indicate that underground water mainly flows from south to north. Therefore, underground water is heated below Mt. Parakasak and flows towards the foot of the mountain. Then the heated water ascends through fractures in the fault systems and discharges at the surface. Discharge temperatures ranging from 50^{o}C to 60^{o}C was obtained in the simulation in the area where the hot springs are present, while temperatures from 25^{o}C to 26^{o}C were obtained where the cold springs occur. The discharge rate from the springs was calculated to be between $3.43x10^{-2}$ m^3/s and $5.79x10^{-2}$ m^3/s.

ACKNOWLEDGEMENTS

The authors wish to thank Cipta E., Febri H., Hendarmawan and Undang M. for the data on electric resistivity surveys in the study area

REFERENCES

Bear J.: Hydraulics of groundwater. *McGraw Hill.* (1979).

Bertani.R.: Geothermal power generation in the world 2005–2010 update report. *Geothermics.* 41. pp1-29. (2011).

Boy Yoseph C.SA., Itoi.R., Taguch.S., Yamashiro.R.: Groundwater Flow System in Mt.Karang West Java, Indonesia Based on the Hydrochemistry of Surface and Ground Waters. *Proc. International Symposium on Earth Science and Technology 2012,* Jalan Tamansari, Indonesia. (2012).

Cipta.E., Febri H., Hendarmawan and Undang M.: Pendugaan nilai tahanan jenis batuan debagai upaya untuk mengetahui struktur geologi yang berkembang pada endapan vulkanik di kec. Padarincang, provinsi banten. *Buletin Sumber Daya Geologi.* 6. pp23-28.(In Indonesian)

De Wiest: Flow Through Porous Media. *Academic Press.* (1969).

Diersch, H.J.G., FEFLOW Reference Manual. Institute for Water Resources Planning and Systems Research Ltd., Berlin, Germany, 278 pp.(2002.)

Fetter.C.W.: Applied Hydrogeology. *Prentice Hall.*(1994).

Fujii.H.,Inatomi.T,Itoi.R.,Uchida.Y.: Development of suitability maps for ground-coupled heat pump systems using groundwater and heat transport models. *Geothermics.* 36. pp459-472. (2007).

Lund.W.J., Freeston.H.D., Boyd.L.T.: Direct utilization of geothermal energy 2010 worldwide review. *Geothermics.* 40. pp159-180. (2011).

Olena, B., Clayton, V.D.: Statistical approach to inverse distance interpolation. *Stochastic Environmental Research and Risk Assessment.* 23. Pp543-553. (2009).